Scanning Microscopy

Volume 2 | Number 1 Article 12

10-19-1987

Junction Electron-Beam-Induced Current Techniques for the Analysis of Photovoltaic Devices

R. J. Matson
Solar Energy Research Institute

Scanning Microscopy, Vol. 2, No. 1, 1988 (Pages 121-127) 0891-7035/88$3.00+.00
Scanning Microscopy International, Chicago (AMF O'Hare), IL 60666 USA

JUNCTION ELECTRON-BEAM-INDUCED CURRENT TECHNIQUES FOR THE ANALYSIS OF PHOTOVOLTAIC DEVICES

R.J. Matson*

Solar Energy Research Institute, 1617 Cole Blvd., Golden, Colorado 80401

(Received for publication March 30, 1987, and in revised form October 19, 1987)

Abstract

A number of useful electron-beam-induced current (EBIC) techniques have evolved through the study of junction behavior in photovoltaic (PV) devices in cross section as a function of light and voltage bias, temperature, and electron beam scanning parameters. The necessary hardware modifications, the techniques themselves, and their applications are presented. In the case of PV devices, light and/or voltage biasing the entire device while electron probing it in cross section permits the observation of the distribution of the narrowing or extension of the space-charge region. Monitoring the junction behavior as a function of temperature has at least two applications. In situ heating of the device in the junction EBIC (JEBIC) mode permits the observation of the rate of movement of the junction further into the material as a function of time and temperature. Through low-temperature studies of cross sections, the change in the material's electrical properties have been recorded and correlated with device I-V and quantum efficiency measurements at these temperatures. Further, the JEBIC profile has been used to predict the quantum efficiency of the device. In the case of thin-film $CdS/CuInSe_2$ devices, newly developed JEBIC techniques have been instrumental in determining the role of oxygen in improving device performance and stability.

Key Words: Electron-Beam-Induced Current, Charge-Collection Microscopy, $CuInSe_2$, Cross-Sectional Electron-Beam Induced Current, Junction Electron-Beam-Induced Current, Photovoltaics

*Address for correspondence:
Richard J. Matson
Solar Energy Research Institute
1617 Cole Blvd.
Golden, CO 80401 Phone No. (303) 231-1126

Introduction

The application of junction electron-beam-induced current (JEBIC) to various semiconductor materials and devices has extended the use of EBIC and resulted in valuable new characterization techniques. This paper is a natural extension of an earlier one published in this series (Matson, 1984), in which many of the hardware modifications to the scanning electron microscope (SEM) necessary to these techniques, along with other techniques, were discussed. As such, the purpose of this paper is to discuss a few additional modifications that have been made and the resulting techniques and applications of the combined EBIC system. Junction, or what otherwise may be called cross-sectional, EBIC involves electron probing of the cleaved cross section, and, therefore, the exposed junction, of a semiconductor device (Fig. 1.). The relatively high energy electron beam serves to locally generate a large number of electron-hole pairs which are subsequently separated and collected, more or less efficiently, depending on their proximity to the device junction. The charges that reach the junction via diffusion or by generation within the junction, are subsequently separated by the intrinsic electric field (space-charge region, SCR). The resulting current is collected via contacts, amplified, and used to Y (deflection) or Z (intensity) modulate the CRT of the SEM, hence the terms electron-beam-induced current (EBIC) or charge-collection microscopy (CCM) (Holt, et al., 1976, Leamy, 1982). (See Fig. 1.) If the electron beam is scanned in a line normal to the junction, the resulting JEBIC line scan can be viewed as a spatial charge-collection efficiency distribution or profile. Plotting the logarithm of the EBIC with distance, the slope (d(lnEBIC)/dx) can be used to determine the minority carrier diffusion length on either side of the junction (Luke, et al, 1985).

Hardware Modifications, Techniques, and Applications

Junction EBIC

A simple, yet very useful, application of JEBIC is to locate the electrical junction of a device with respect to the metallurgical

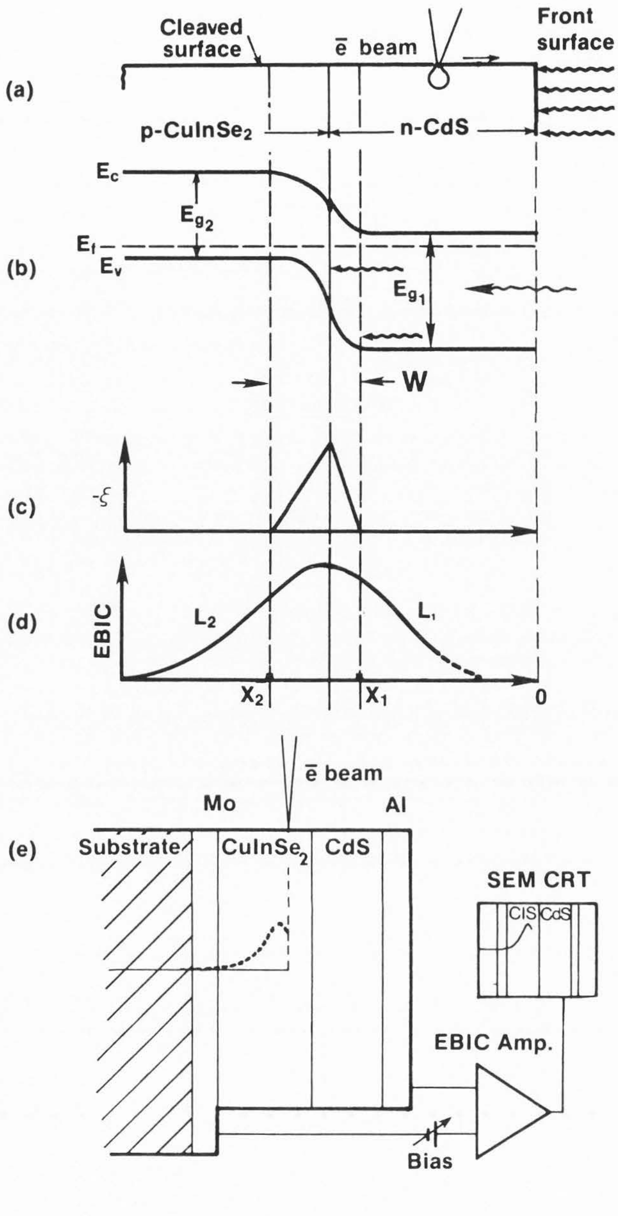

Figure 1: (a) Diagram depicting an electron beam scanning normal to the cross section of a semiconductor device near the junction. The high energy electrons act as a highly localized source of electron-hole pairs. (b) Diagram of an idealized energy band diagram for a heterojunction with a window layer (n-CdS) and an absorber layer (p-$CuInSe_2$) and the corresponding SCR of width W. (c) The corresponding intrinsic electric field. (d) The charge collection (EBIC) profile resulting from scanning the beam across the junction area. X_1 and X_2 denote the SCR limits, and L_1 and L_2 the minority carrier diffusion lengths. (e) The EBIC is collected through ohmic contacts, amplified, and used to modulate the SEM CRT.

junction, in the case of heterojunction devices, or with respect to the surface, in the case of homojunction devices. Figure 2 illustrates an example of a homojunction which in fact was intended as, or thought to be, a heterojunction between the n-CdS and the p-$CuInSe_2$ material. The evident difference in topography is due to the CdS being a polycrystalline thin film and the $CuInSe_2$ being single crystal. This particular case was significant because it served to show that depositing CdS onto $CuInSe_2$ resulted in the type conversion of the surface of the $CuInSe_2$ from p-type to n-type, resulting, in turn, in the formation of a homojunction in the $CuInSe_2$ (Matson, et al., 1987). Figure 2 is a superposition of both an EBIC line scan and an EBIC image on the secondary electron image (SEI) of the cross section of the device. The JEBIC line scan is used to assign a junction depth, usually at the EBIC peak position, and to obtain a good idea of both the space-charge-region width (W) and the minority carrier diffusion length (L). W and L are more accurately determined by digitally stepping the electron beam across the junction, recording the JEBIC(x), and applying a least-squares fit to the plot of ln(JEBIC(x)) (Partain and Shea, 1979, van Roosbroeck, 1955, and Luke et al., 1985). In terms of determining the SCR width from the JEBIC line scan, a comparison between W measured from capacitance-voltage (C-V) measurements and that estimated from the JEBIC profiles of the same devices over the years have shown good agreement. The superposition of the EBIC image and the SEI allows the location and spatial distribution of the electrical activity with respect to the intended junction location to be recorded.

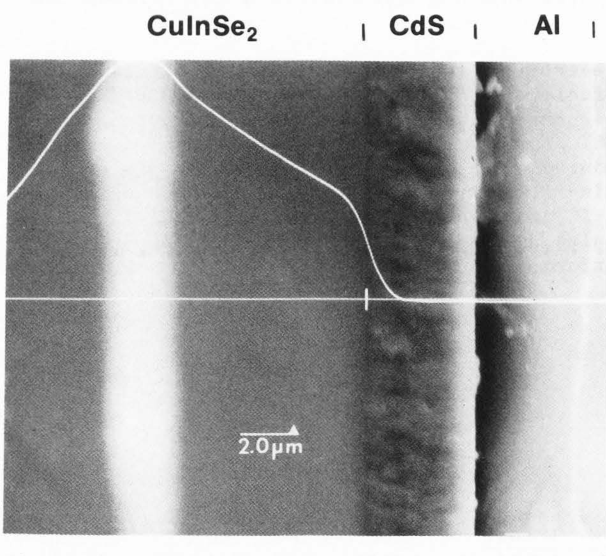

Figure 2: Combined EBIC and SEI micrograph of polycrystalline thin film CdS on single crystal $CuInSe_2$ with an EBIC line scan. The horizontal line indicates both where the electron beam was scanned and the zero beam current reference line. The white (EBIC) band represents the spatial variation in electrical activity. Through differential amplification, just the peak response is imaged. (See Matson et al., 1987).

In addition, the quantum efficiency (QE) of photovoltaic devices has been calculated from the relation

$$QE = \alpha\int_{o}^{x_1} e^{-\alpha x}\cdot e^{-(x_1-x)/L_1}\,dx + \alpha\int_{x_1}^{x_2} e^{-\alpha x}dx + \alpha\int_{x_2}^{d} e^{-\alpha x}\cdot e^{-(x-x_2)/L_2}\,dx$$

$$= \left(\frac{\alpha L_1}{\alpha L_1-1}\right)e^{-x_1/L_1} - \left(\frac{1}{\alpha L_1-1}\right)e^{-\alpha x_1} - \left(\frac{1}{\alpha L_2+1}\right)e^{-\alpha x_2} - \left(\frac{\alpha L_2}{\alpha L_2+1}\right)e - \left(\frac{x_2}{L_2} + \alpha d + \frac{d}{L_2}\right) \quad (1)$$

and from knowledge of the absorption coefficient as a function of wavelength, $\alpha(\lambda)$, and the JEBIC profile, which can be used to determine the minority-carrier diffusion lengths, L_1 and L_2, the SCR limits, X_1 and X_2, as depicted in Fig. 1. (Matson, et al., 1987). In principle, the $\alpha(\lambda)$ could be determined from the measured QE and the JEBIC line scan.

Low-Temperature JEBIC

An earlier paper (Matson, 1984) described most of the hardware modifications necessary to perform temperature-dependent JEBIC from 80°K to 720°K. The only additional modification recommended is to machine an insert for the original sample holder for the cold stage (Matson, 1984, Fig. 3b) to permit edge-on viewing directly analogous to the insert for the hot stage (Matson 1984, Fig. 2b), intended for the same purpose.

Applications of temperature-dependent planar EBIC have been reported in the literature. In particular, the analysis of EBIC contrast as a function of lower temperatures has been used to study the electrical properties of individual dislocations of different character (Boyes, et al., 1982; Breitenstein and Heydenreich, 1983; Ourmazd, et al., 1983). Low temperature JEBIC has been used before to study the temperature dependence of the minority carrier diffusion length in lead chalcogenides (Eisenbeiss, et al., 1984). Our only application to date has been the examination of the low-temperature characteristics of $CdS/CuInSe_2$ diodes in which the large number of traps are unevenly distributed through the depth of the layered $CuInSe_2$ structure. Hence, the shift of the locus or position of the electrical activity (the junction) depends on the Fermi level (temperature dependent) and the electrical bias on the sample. At lower temperatures, the junction not only shifts away from the heteroface towards the back contact but reverses current direction (polarity) at a forward bias equal to that of the open-circuit voltage (Fig. 3). The EBIC signature correlated well with I-V and quantum efficiency (QE) under the same conditions in that the I-V showed double-junction behavior and the QE showed both the expected spectral dependence of a buried junction and the current reversal. The JEBIC supported this by showing the locations in the film where these type conversions were taking place and ultimately provides clues to the defect chemistry determining the electrical properties of the $CuInSe_2$.

In principle, the low-temperature JEBIC stage can be extended to scanning deep level transient spectroscopy (SDLTS) (Breitenstein and Heydenreich, 1983) in cross section where the spatial distribution of defects in layered devices may be imaged.

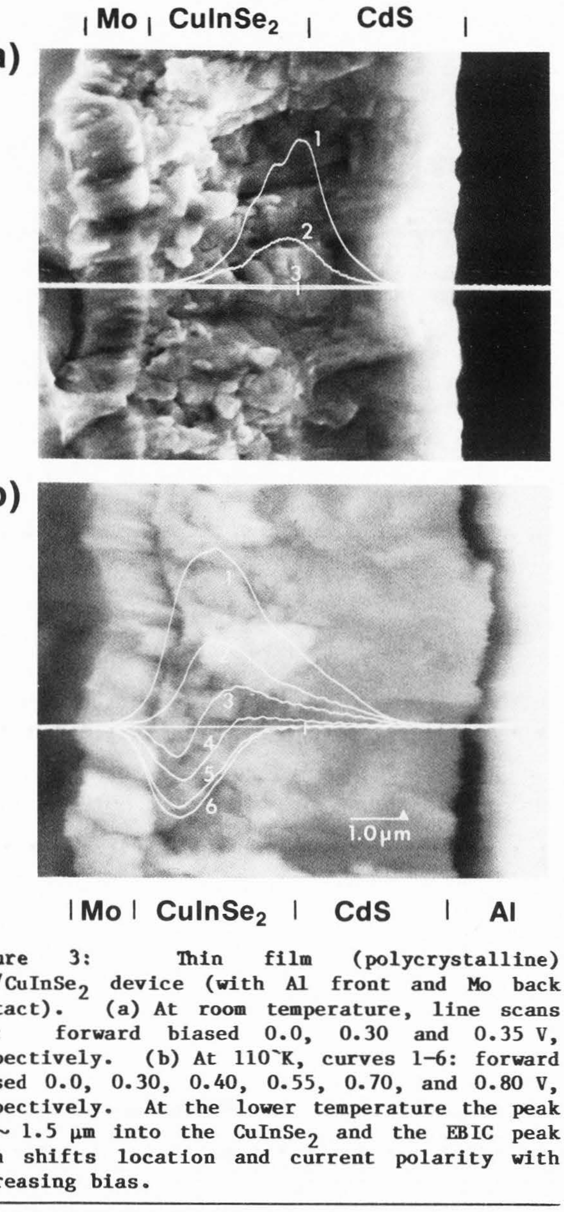

Figure 3: Thin film (polycrystalline) $CdS/CuInSe_2$ device (with Al front and Mo back contact). (a) At room temperature, line scans 1-3: forward biased 0.0, 0.30 and 0.35 V, respectively. (b) At 110°K, curves 1-6: forward biased 0.0, 0.30, 0.40, 0.55, 0.70, and 0.80 V, respectively. At the lower temperature the peak is ~ 1.5 μm into the $CuInSe_2$ and the EBIC peak both shifts location and current polarity with increasing bias.

High-Temperature JEBIC

This method is complicated by two factors. First, the device performance degrades significantly with higher temperatures, so that obtaining a signal may be problematic. In this case, the heating or annealing effects may be assessed by letting the sample cool back down before performing the EBIC measurement. Secondly, the hot stage expands, with heating, resulting in sample movement. This can be addressed in most cases by allowing the system to come to thermal equilibrium before recording the EBIC information.

One application for an EBIC hot stage is to measure the depth of the junction from the surface as a function of annealing time and temperature and using this to determine the diffusivity (Grove, 1967). Another is to monitor the change in a material's electrical properties with temperature. A case in point is noted in thin-film CdS/CdTe, CdS/Cu_2S, and CdS/$CuInSe_2$ devices, where post-deposition heat treatments are known to improve device performance (Matson, et al., 1986). In the case of CdS/$CuInSe_2$, these techniques were used to argue that the effect of the heat treatment was on the $CuInSe_2$, as opposed to the CdS, and that the heating resulted in the type conversion of the $CuInSe_2$ through the incorporation of oxygen and a consequent progression of the junction toward the heteroface (Matson et al, 1986).

Biased JEBIC

To perform light- and/or voltage-biased JEBIC, beam blanking and a lock-in amplifier with a current-to-voltage pre-amplifier are required due to the current resulting from biasing the sample easily saturating most current amplifiers and swamping the EBIC signal. The lock-in amplifier separates the modulated EBIC signal from the D.C. bias current. In the present system, a PAR Model 124-A Lock-In Amplifier with a Model 184 Current Sensitive Pre-Amplifier is used. Although most, or all, lock-in amplifiers are suitable for slow line scans, their system response times are too slow for EBIC imaging. Voltage biasing requires a reasonably noise-free voltage source. A battery and voltage divider network is both simple and effective.

Light-Biased JEBIC

Light biasing of the sample with the light directed normal, or slightly off-normal, to the device, noted in Figures 1a,b, is accomplished via a fiber optic cable mounted in the SEM sample chamber. The fiber optic cable, with a vacuum feed-through, in contrast to just a light source inside the SEM vacuum chamber, allows variable wavelength, variable intensity, and collimated light to be applied to the sample. We found that a fiber optic cable, snugly fed through a suitably sized rubber cork which was in turn used in a spare port in the SEM (a JEOL JSM-35c), all with ample vacuum grease appropriately applied, functioned quite adequately as a vacuum feed-through for the cable.

This arrangement allows the junction behavior to be studied under actual operating conditions. This technique is especially applicable to devices in which the superposition principle does not hold or, otherwise, in which the charge-collection distribution is thought to differ under light-biased conditions from that of dark conditions. In photovoltaic systems, amorphous Si, CdS/CdTe, CdS/Cu_2S, and CdS/$CuInSe_2$ devices are candidates. An application of temperature dependent, light biased EBIC which could be easily extended to JEBIC, involves the photo-induced modulation of the EBIC through the use of chopped sub-bandgap monochromatic light to study the photo-ionization of deep levels with high spatial resolution (Li, et al, 1986).

Voltage-Biased JEBIC

The hardware requirements were addressed above. One application of this technique is to record the distribution of SCR depletion or widening with the application of either reverse or forward biasing, respectively, as shown in Fig. 4. This can be used in fundamental device studies to complement C-V measurements which can determine the SCR width but neither the junction location nor the spatial distribution of the SCR, which may be useful in modeling complex device structures. Another application is bias dependent electron-beam-induced-conductivity characterization of non-uniformities in insulating materials such as zinc oxide ceramics (Bernds, et al., 1984) and Si_3N_4 on Si (Matson, et al., to be published).

JEBIC "Shift"

Through investigations of the role of the post-deposition oxygen treatment on thin-film CdS/$CuInSe_2$ solar cells, it was determined that the device was a homojunction rather than the expected heterojunction. A full report has been presented elsewhere (Matson, et al., 1986). For present purposes, the more interesting phenomenon was the shift in the EBIC profile with successive scans. That is, the sample was positioned and aligned such that the first EBIC line scan could be performed on an area of the sample with no pre-exposure to the electron beam--a so-called "virgin" line scan. This was followed by a succession of line scans wherein the change in the EBIC line scan was monitored until it stabilized and no further change occurred at which point the line scan was recorded--the so-called "final" line scan (Fig. 5). Through the application of this "virgin" EBIC line scan technique to samples of varying composition and fabrication techniques and post-deposition heat and oxidation/reduction treatment, it was discovered that the electron beam had an effect on the $CuInSe_2$ analogous to that of chemical reducing agents. Further, it was found that the oxygen served to type-convert the outer layer of $CuInSe_2$, thereby shifting the junction closer to the heteroface, and that the electron beam served to probe the stability of the incorporation of the oxygen (Matson et al, 1986) because the EBIC shift corresponded to oxygen removal by the beam. Recent scanning Auger studies of the threshold for the electron stimulated desorption (ESD) of oxygen from thin film $CuInSe_2$ (Nelson, et al., 1987) and calculations of injected charge densities have shown that even under moderate beam conditions (20kV, 50pA, 100Å beam diameter) the SEM probe can dislodge oxygen. In short, the electron beam was the central tool in determining the role of oxygen in this material system. Because of the parallels between this system and CdS/CdTe, CdS/Cu_2S and related compounds, it is reasonable to try to extend the use of these techniques to these other materials systems.

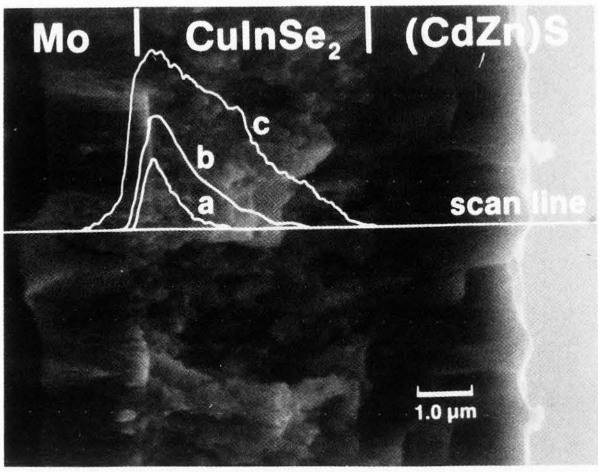

Figure 4: The effect of forward bias (a), zero bias (b), and reverse bias (c) on a thin film $CdS/CuInSe_2$ device with a junction buried deeply enough in the $CuInSe_2$ to be considered a $Mo/CuInSe_2$ Schottky barrier (Russel et al., 1982). The corresponding SCR extension (c) and contraction (a) appears evident.

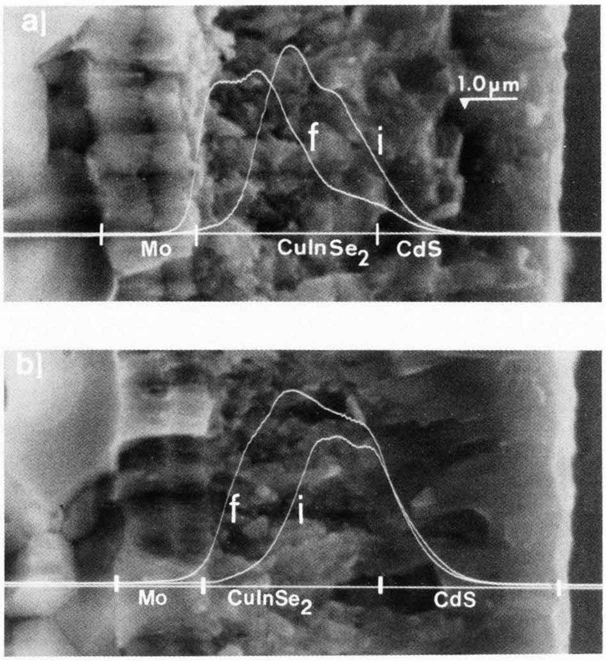

Figure 5: Comparison of the initial (i) and final (f) line scans before (a) and after (b) post-deposition heat (in oxygen) treatment. The $CdS/CuInSe_2$ heteroface is denoted by tick marks. This comparison shows the change of the location and distribution of electrical activity and sensitivity to the electron beam before and after treatment. (See Matson et al., (1986).

Summary/Conclusion

The hardware modifications for low- and high-temperature, light- and voltage-biased, planar and junction EBIC were discussed. Associated techniques and some applications have also been presented for the junction EBIC case, including some more specific to thin-film $CdS/CuInSe_2$ and analogous devices. In general, the purpose was to suggest a few EBIC hardware modifications, techniques and applications that could serve to extend the already formidable array of SEM-based semiconductor characterization tools. Readers interested in further details may contact the author.

Acknowledgements

The author wishes to thank R. Noufi, M.M. Al-Jassim, L.L. Kazmerski, A.J. Nelson (all of SERI), and A. Rothwarf (Drexel University) for their contributions to this effort. This work was supported under U.S. Department of Energy contract number DE-AC02-83CH10093.

References

Boyes ED, Dixon-Brown G, Ourmazd A (1982). A system for EBIC analysis of defects using controlled low temperatures in the SEM. Electron microscopy and Analysis, 1981, Proceedings of the Institute of Physics Electron Microscopy and Analysis Group Conference, U. Cambridge, Sept., 1981, MJ Goringe, (ed.), Inst. Phys. Conf. 61, ch. 11:517-518.

Bernds A, Löhnert K, Kubalek E (1984). SEM EBIC investigations of ZnO varistor ceramics. J. DePhys. 45, C2, 861-864.

Breitenstein O, Heydenreich JM (1983). Combined electron microscopical and DLTS (ESP,DSLTS) investigations in semiconductors. J. Phys. Colloq. 44(C4):207-215.

Eisenbeiss A, Heinrich H, Jakubowicz A, Maurer W, Palmetshofer L, Prier HM, Bachem KH, Böttner H (1984). Investigations of diffusion length and lifetime in lead chalcogenides by electron-beam-induced current measurements at low temperature, J. Appl. Phys. 56, 362-367.

Grove AS (1967). Physics and Technology of Semiconductor Devices. Wiley & Sons, NY: 35-90.

Holt DB, Muir MD, Grant PR, Boswara IM (1976). Quantitative Scanning Electron Microscopy, Academic Press, Inc., NY:213-287.

Leamy HJ (1982). Charge collection scanning electron microscopy, J. Appl. Phys. 53(6):R51-R80.

Li CJ, Sun Q, Lagowski J, Gatos HC (1986). EBIC spectroscopy - A new approach to microscale characterization of deep levels in semi-insulating GaAs, Mat. Res. Soc. Symp. Proc. 46, 441-446.

Luke KL, von Roos O, Cheng L (1985). Quantification of the effects of generation volume, surface recombination velocity, and diffusion length on the electron-beam-induced current and its derivative: determination of diffusion lengths in the low micron and submicron ranges. J. Appl. Phys. 57(6):1978-1984.

Matson RJ (1984). Scanning electron microscope modifications for electron beam induced current analysis with applications to photovoltaic materials and devices. Scanning Electron Microsc. 1984; II:625-632.

Matson RJ, Noufi R, Ahrenkiel RK, Powell RS (1986). EBIC investigations of junction activity and the role of oxygen in $CdS/CuInSe_2$ devices. Solar Cells 16:495-519.

Matson RJ, Noufi R, Bachmann KJ, Cahen D (1987). CdS induced homojunction formation in crystalline p-$CuInSe_2$. Appl. Phys. Lett. 50:158-160.

Nelson AJ, Burnham NA, Swartzlander AB, Asher SE, Kazmerski LL, Ireland PJ (1987). Analysis of $CuInSe_2$: Electron and ion beam effects. Proc. 19th IEEE Photovoltaic Specialists Conference, New Orleans, May 1987, (In-press).

Noufi R, Powell RC, Matson RJ (1987). On the effects of stoichiometry and oxygen on the properties of $CuInSe_2$ thin films and devices. Solar Cells 21, 55-63.

Ourmazd A, Wilshaw PR, Booker GR (1983). The temperature dependence of EBIC contrast from defects. Proceedings of the 41st Annual Meeting of the Electron Microscopy Society of America, GW Bailey, (ed.), San Francisco Press:142-145.

Partain LD, Shea SP (1979). Obtaining accurate values of diffusion length with the scanning electron microscope. Proc. of CEC 2nd EC Photovoltaic Solar Energy Conference (West Berlin, April 1979) D Reidel, London, Van Overstraeten R, Poly W (eds.) 639-646.

Russel PE, Jamjoum O, Ahrenkiel RK, Kazmerski LL, Michelsen RA, Chen, WS (1982), Properties of the Mo-$CuInSe_2$ interface, Appl. Phys. Lett. 40, 995-997.

Van Roosbroeck W (1955). Injected current carrier transport in a semi-infinite semiconductor and the determination of lifetimes and surface recombination velocities, J. Appl. Phys. 26, 380-391.

Zurcher P, Nelson AJ, Johnson P, Lapeyre GJ, Noufi R (1987). Soft X-ray photoemission investigation of the oxidation of $CuInSe_2$ thin films, Proceedings of the 19th IEEE Photovoltaic Specialists Conference, New Orleans, May 1987, (in-press).

Discussion with Reviewers

J. Heydenreich: In some cases relative to the conventional EBIC method the technique of time-resolved EBIC (TREBIC) enables additional information to be gained. What about the application of this technique to the analysis of photovoltaic devices?

Author: The advantage of TREBIC is working with long lifetime materials, such as Si, and improved EBIC spatial resolution. This is a short lifetime (submicrosecond) material and improved spatial resolution of JEBIC peak position was gained by use of differential EBIC (DEBIC) techniques. Hence, although TREBIC has clear application to Si based devices, there is not an apparent advantage in this material system.

D. Köhler: Did you observe any differences in the results of the JEBIC and light-biased JEBIC measurements?

Author: No, not in JEBIC peak location or profile. The object of these experiments was to determine if the effect of light on the quite photoconductively sensitive CdS would, in turn, affect the location of the JEBIC peak in thin film $CdS/CuInSe_2$ samples. Due to the number, variety and lifetimes of traps in this material system, the expected effect of light biasing on the space charge region (SCR) width at short circuit conditions is unclear. A better test for light bias effects on the SCR would be to monitor JEBIV on a simpler material system.

J. Heydenreich: In the light-biased JEBIC, the charge collection distribution is a function of the wavelength and of the intensity of the light used. Under which experimental conditions have the experiments been carried out and which results have been achieved?

Author: An ELH type lamp, whose output is reasonably well spectrally matched to that of terrestrial sunlight, was used as the light source. The intensity at the sample was adjusted for one sun conditions (100 mW/cm^2).

As noted above, the results were unclear, probably due to the complexity of the material system.

J.D. Meakin: A number of the figures appear to show substantial response from well within the Mo layer (e.g., Fig. 4). Please comment on the precision with which the EBIC scans and SEM images are superposed.

Author: By the routine superposition of SEI and SEI line scans of NBS magnification standards, we know that the superposition of the two and the magnification scale remains exact ($<$ 1% error). The EBIC response observed in the Mo is a result of the generation volume due to electron scattering within the material.

J.D. Meakin: You report that irradiation during EBIC moves the position of the junction (Fig. 5) so that presumably even the initial line scan is suspect. The $CdS/CuInSe_2$ junction is also somewhat indistinct. Taking these two facts together, would you estimate the lateral uncertainty in the relative position of the "true" EBIC peak and the metallurgical junction for an optimized operating cell?

Author: An extensive array of tests for electron beam artifacts on this material were performed to address this very question; the more important of which were noted in Matson et al., 1986. For example, because the effect is dose related, we examined beam currents from $2x10^{-14}$A to $2x10^{-7}$A (measured with a Keithley 642 electrometer and Faraday cup) and beam voltages from 10kV to 40kV.

Concerning the issue of the virgin, or initial, line scan truly characterizing the actual device junction or not, the rate at which the JEBIC profile evolves with successive scans of the electron beam appears to be the best measure. That is, if the profile changes substantially between the first and second scans, as opposed to after many scans, the initial line scan becomes suspect. But what has been observed over many samples, before and after oxygen treatment, is a slow evolution. This, and the fact that at even very low dosages ($2x10^{-14}$A), the initial peak is in the same position, clearly indicates that a first scan is correct.

Accurately identifying the metallurgical interface is a little more problematic. The thickness of the $CuInSe_2$ layer is evaluated at several points with the SEM where the CdS has been removed and compared with surface profilometer results. Also, the $CuInSe_2$ and CdS generally have different grain sizes and structure. These and consistency with other clues derived from the SEI are the basis for assigning the position of the heteroface.

Overall the estimated lateral uncertainty, including effects of differences in bandgaps of the two materials, is probably no worse than 0.2 μm.

J.D. Meakin: There are potential artifacts using lock-in amplification for making either collection efficiency or EBIC measurements with an applied voltage bias. For example, (1) an apparent light generated current can be detected in QE measurements on samples containing no active junction but merely a photoconductive component. (2) A spurious reversal of QE response from a photovoltaic device has also been observed and traced to a finite out-of-phase component in the amplified signal. Can such effects be discounted for the reported current reversals?

Author: Referring to the experiment represented in Fig. 3; first, concerning the "apparent" existence of a junction where there is none, we are assured by generation factors ($EBIC/I_b$) $\geq$1000 that charge separation, and hence a junction, is present. Second, because of the observed effect of biasing on the phase relation in the lock-in signal, the phase was checked, and adjusted as necessary, with each line scan. Further, as noted in the text, the biased low temperature quantum efficiency measurements clearly corroborated the observed junction position and current reversal. Hence, we believe that the characterization is correct.

J. Heydenreich: The electrical activity of the $CdS/CuInSe_2$ junction does, of course, strongly depend on the geometrical (morphological structure of the interface region). Is there a detailed knowledge of the transition region (including the characterization of existing defects in the boundary), revealed e.g., by cross-sectional TEM?

Author: No, to my knowledge very little cross-sectional TEM of the $CdS/CuInSe_2$ heteroface has been done. However, as noted in this report, the active device junction occurs well within the $CuInSe_2$, therefore presumably obviating this kind of investigation. However, photoluminescence studies of $CuInSe_2$, with and without the CdS window layer, are in progress which will examine surface defect states.

H. Matsunami: Does Mo work as a good ohmic contact to $CuInSe_2$ at low temperatures?

Author: Although the $CdS/CuInSe_2$ device I-V characteristics clearly indicate double diode behavior the JEBIC, the measured spectral response, and the corresponding absorption coefficients all indicate that the second junction is near (within 1.0μm of, but not at) the $Mo/CuInSe_2$ interface. From this we conclude that rectifying behavior is not developing at that interface at lower temperatures, without being able to comment on the resistivity of the contact itself.

H. Matsunami: As an experimental result, oxygen type converts $CuInSe_2$. Is there any evidence that oxygen functions as a donor in $CuInSe_2$ to type convert the material?

Author: No. The type conversion is from n-type to p-type through the passivation, or elimination, of donor type defects by the oxygen. The reader is referred to Matson et al., 1986, Zurcher et al., 1987, and Noufi et al., 1987 for further details.